5-1-1997

Whole Earth Telescope Observations of the Helium Interacting Binary PG 1346+082 (CR Bootis)

Judith L. Provencal
University of Texas at Austin

Donald E. Winget
University of Texas at Austin

R. Edward Nather
University of Texas at Austin

Edward L. Robinson
University of Texas at Austin

J. Christopher Clemens
California Institute of Technology

See next page for additional authors

THE ASTROPHYSICAL JOURNAL, 480:383–394, 1997 May 1

WHOLE EARTH TELESCOPE OBSERVATIONS OF THE HELIUM INTERACTING BINARY PG 1346+082 (CR BOOTIS)

J. L. PROVENCAL[1,2] D. E. WINGET,[1] R. E. NATHER,[1] E. L. ROBINSON,[1] J. C. CLEMENS,[3,4]
P. A. BRADLEY,[5] C. F. CLAVER,[6] S. J. KLEINMAN,[7] A. D. GRAUER,[8,9] B. P. HINE,[10,11]
L. FERRARIO,[12] D. O'DONOGHUE,[13] B. WARNER,[13] G. VAUCLAIR,[14] M. CHEVRETON,[15]
S. O. KEPLER,[16,17] M. A. WOOD,[18] AND G. W. HENRY[17,19]

Received 1996 September 30; accepted 1996 November 19

ABSTRACT

We present our analysis of 240 hr of white-light, high-speed photometry of the dwarf nova–like helium variable PG 1346+082 (CR Boo). We identify two frequencies in the low-state power spectrum, at 679.670 ± 0.004 μHz and 669.887 ± 0.008 μHz. The 679.670 μHz variation is coherent over at least a 2 week time span, the first demonstration of a phase-coherent photometric variation in any dwarf nova–like interacting binary white dwarf system. The high-state power spectrum contains a complex fundamental with a frequency similar, but not identical, to the low-state spectrum, and a series of harmonics not detected in low state. We also uncover an unexpected dependence of the high-frequency power's amplitude and frequency structure on overall system magnitude. We discuss these findings in light of the general AM CVn system model, particularly the implications of the high-order harmonics on future studies of disk structure, mass transfer, and disk viscosity.

Subject headings: stars: individual (PG 1346+082) — stars: oscillations — white dwarfs

1. INTRODUCTION

PG 1346+082 (CR Boo) is a member of a special subset of short-period binary systems, the interacting binary white dwarfs (IBWDs). IBWDs, also known as AM CVn stars, after the prototype, contain two white dwarfs of extreme mass ratio in close proximity. The secondary, with an estimated mass ranging from 0.02 to 0.09 $M_\odot$, fills its Roche lobe and transfers material to the much more massive primary via an accretion disk (Faulkner, Flannery, & Warner 1972). IBWDs are fascinating laboratories of accretion dynamics. Recent spectroscopic evidence argues that the prototype, AM CVn, contains a stable accretion disk with a 13.4 hr precession period (Patterson, Halpern, & Shambrook 1993). AM CVn stars also provide insight into binary star evolution, while offering an unique opportunity to peer into a stellar core remnant and directly view the by-products of nucleosynthesis (Marsh, Horne, & Rosen 1991). The extremely low secondary mass suggests the donated material originates from a present surface, once deep within the core of the progenitor main-sequence star. Yet spectra of all AM CVn stars are helium-rich, rather than carbon-dominated, indicating that the evolutionary path traversed by these systems precludes the ignition of helium in the core of the secondary progenitor. Helium-core white dwarfs created by single-star evolution could not have yet formed in the age of the Galactic disk (Winget et al. 1987).

In addition, the AM CVn stars offer a possible channel onto the white dwarf cooling track. Recent theoretical and observational work (see Fontaine & Wesemael 1996 for a review) argues that most, if not all, hydrogen-surface white dwarfs (DAs), which comprise 80% of the total white dwarf population, have thick ($\approx 10^{-4}$ $M_\odot$) surface layers, and comprise a fairly well-understood channel of white dwarf evolution. The situation is less clear for helium-surface white dwarfs (DBs), which comprise the remaining 20% of the population. Observational evidence suggests a range of helium layer thicknesses, which could be explained through either time-dependent diffusion (Dehner & Kawaler 1995; Provencal et al. 1996) or multiple sources for DBs, such as the subdwarfs, the DAO stars, and the AM CVn systems (Shipman 1996). Evidence abounds for an evolutionary trend between orbital separation and accretion rate among the six AM CVn objects (Table 1) (Provencal 1994). The mass transfer will not stop until the secondary is completely absorbed, leaving a solitary DB (Nather, Robinson, & Stover 1981), perhaps providing a significant fraction of the field DBs we observe today.

The Palomar Green survey (Green, Schmidt, & Liebert 1986) object PG 1346+082 (CR Boo), one of three dwarf nova–like AM CVn systems, undergoes outbursts ranging from a low-state (minimum light) magnitude of ≈17.4 (m_b)

[1] Department of Astronomy and McDonald Observatory, University of Texas, Austin, TX 78712; jlp@chopin.udel.edu.
[2] Department of Physics and Astronomy, University of Delaware, Newark, DE 19716.
[3] Division of Physics, Mathematics, & Astronomy, California Institute of Technology, Pasadena, CA 91125.
[4] Hubble Fellow.
[5] XTA MS B220, Los Alamos National Laboratory, Los Alamos, NM 87545.
[6] Kitt Peak National Observatory, NOAO, Tucson, AZ 85726-6732.
[7] Big Bear Solar Observatory, Big Bear City, CA.
[8] Department of Physics and Astronomy, University of Arkansas, 2801 South University Avenue, Little Rock, AR 72204.
[9] Guest Observer, Siding Spring Observatory, Australia.
[10] NASA Ames Research Center, M.S. 244-4, Moffett Field, CA 94035.
[11] Visiting Astronomer, Institute for Astronomy, Honolulu, HI.
[12] Australian National University, Canberra, Australia.
[13] Department of Astronomy, University of Cape Town, Rondebosch 7700, South Africa.
[14] Observatoire Midi-Pyrenees, 14 Avenue E. Belin, 31400 Toulouse, France.
[15] Observatoire de Paris-Meudon, F-92195 Meudon, Principal Cedex, France.
[16] Instituto de Fisica, Universidade Federal do Rio Grande do Sul, 91501-970 Porto Alegre-RS, Brazil.
[17] Visiting Astronomer, Cerro Tololo Inter-American Observatory.
[18] Department of Physics and Space Sciences, Florida Institute of Technology, 150 West University Boulevard, Melbourne, FL 32901.
[19] Center for Excellence in Information Systems, Tennessee State University, 330 10th Avenue North, Nashville, TN 37203.

TABLE 1

THE INTERACTING BINARY WHITE DWARF SYSTEMS

Name	Temp (K)	Magnitude (*B*)	Period (s)	Amplitude (mmi)	Spectrum
AM CVn	25000	13.9	1011.4	11 − <3	Absorption
			525.6	11	
			350.4	3.2	
EC 15330−1403		13.6	1119	≈18	Absorption
PG 1346+082 (CR Boo)	20000 (h)	13.6–17.3	1471.3	55 (l) < 5 (h)	Absorption (h)
			1492.8	32 (l) < 7 (h)	Weak emission (l)
V803 Cen	20000 (h)	13.4–17.4	1600	20	Absorption (h)
	15000 (l)		175		Emission (l)
CP Eri		≈16.7–21	1800	68 (l) 16 (h)	Absorption (h)
G61-29	≤10000 (disk)	15.8	2790	<3	Emission

NOTE.—PG 1346+082, V803 Cen, and CP Eri are dwarf nova–like systems. The two letters (l) and (h) denote low- and high-state values.

to a high-state (maximum brightness) magnitude of ≈13.6 (m_b) on a quasi-periodic timescale of 4–5 days (Wood et al. 1987, hereafter W87). PG 1346+082 is also a short-period photometric variable, with high-frequency variations, ≈680 μHz, superposed on the large-scale outbursts (Nather et al. 1984). W87 find the character of the light curve to be correlated with its mean magnitude. Their high-state Fourier transform (FT) is dominated by an unresolved band of power at 680 μHz and its associated harmonics, while their low-state light curve contains flickering, a classic signature of mass transfer (Shafter & Szkody 1984). W87 note that the 680 μHz variation displays a coherency timescale of about 1 week, and they detect evidence of a 2.8 hr variation.

PG 1346+082's key optical spectral characteristics are the common signatures of all AM CVn stars, namely a complete lack of hydrogen and the dominance of neutral helium. In high state, PG 1346+082's optical spectrum contains broad, shallow He I absorption features, consistent with either pressure broadening in the atmosphere of a compact object, or a combination of pressure broadening and Doppler broadening in a swiftly rotating accretion disk (W87). The low-state spectrum is essentially featureless, with the possible exception of weak He I emission at 4471 Å (W87). This behavior is reminiscent of hydrogen-dominated dwarf novae, with absorption features observed during outburst and emission features during minimum light (Wade & Ward 1985).

We chose PG 1346+082 as a target for the Whole Earth Telescope (WET), an international collaboration of astronomers around the globe striving to obtain continuous observations of a target star (Nather et al. 1990), for a number of reasons. First, its complicated small and large amplitude variations, combined with the possibility of multiple, closely spaced frequencies, produce an impossibly tangled alias "web" that cannot be resolved by any amount of single-site data. Second, of the dwarf nova–like AM CVn stars, this particular object is one of the brightest, and it is best situated for an intensive global observational effort. Also, its short-period variations appear more stable than those of V803 Cen, the remaining bright dwarf nova–like AM CVn system (O'Donoghue et al. 1994).

With this work, we will build on the results of W87 and investigate unanswered questions surrounding PG 1346+082's photometric behavior. W87 were unable to resolve the 680 μHz power band and identify individual frequencies. We do not know if this band represents the system's orbital frequency, if it represents a single unstable frequency or multiple variations, where within the system the variations arise, or what role the high-state harmonics play. It is particularly important that we positively identify the orbital period. Only G61-29 has had its orbital period unambiguously identified (Nather et al. 1981). Studies of the remaining systems usually assume the orbital period to be in some way related to the photometric period (Patterson et al. 1992). We report the results of our observations.

2. DATA ACQUISITION AND REDUCTION

Our observations consist of nearly 240 hr of white-light, high-speed photometry, spanning 15 days during 1988 March. The contributing sites and telescopes are listed in Table 2. As a historical note, this data set represents the inaugural run of WET. Table 2 contains only six participating sites: WET has since grown to include as many as 13 observing sites.

With the exception of South Africa, all data were taken with two-channel photometers (Nather 1973), continuously monitoring a comparison star to verify photometric conditions. South Africa experienced technical difficulties with their second channel; therefore, their data are single-channel only. The light curves are interrupted at irregular intervals of a half-hour to an hour, depending on conditions, to sample sky brightness. All individual runs employ either 10 s or 6 s integration times.

The entire WET reduced light curve is given in Figure 1. We follow the data reduction techniques described by Nather et al. (1990) to remove sky and extinction effects, resulting in light curves expressed in units of fractional amplitude of the total intensity (Fig. 2). Because we divide each light curve by its mean count rate and subtract 1, we lose all mean magnitude information in our reduced light curves. However, each site observed several standard stars on various occasions, and this important information is retrievable (Fig. 3). We made no attempt to weigh individual runs by telescope aperture, and we did not taper the individual light curves. Tapering decreases alias amplitude, but also reduces frequency resolution, which is our main goal. Our extensive observing coverage substantially reduces aliases of itself, rendering tapering unnecessary.

We have traditionally used the unit "mmg" (millimagnitude) to describe relative amplitudes of variations measured in light curves and FTs (see Winget et al. 1991 for an example). However, the term "magnitude" implies a logarithmic scale, while we measure linear, relative, fractional intensities and amplitudes. We will follow

TABLE 2

TABLE OF OBSERVATIONS

Run Name	Telescope	Run Start from T_z (s)	Length (hr)	Interval (s)	Magnitude ($\pm$0.4)
ren-0018	Texas 2.1 m	0	1.77	10	15.3
ren-0019	Texas 2.1 m	8913	1.87	10	15.3
a3.....	Australia 1.0 m	28900	4.06	10	15.6
ren-0022	Texas 2.1 m	87658	5.60	10	15.4
ren-0024	Texas 2.1 m	170328	6.07	10	15.4
tol-0005	CTIO 1.5 m	250072	4.93	10	16.7
ren-0026	Texas 2.1 m	256137	4.28	10	16.7
bph67	Hawaii 0.6 m	275488	4.33	10	16.5
a10	Australia 1.0 m	285175	4.97	10	16.3
s4227	SA 1.0 m	319115	4.07	10	16.3
gv-006.....	France 1.9 m	319921	4.40	6	16.3
tol-0011	CTIO 1.5 m	334496	5.63	10	17.5
ren-0028	Texas 2.1 m	343739	5.93	10	17.4
bph68	Hawaii 0.6 m	355831	5.97	10	17.6
a11	Australia 1.0 m	372058	4.77	10	17.8
gv-008.....	France 1.9 m	406385	5.23	6	17.5
tol-0017	CTIO 1.5 m	423720	2.66	10	17.8
a14	Australia 1.0 m	461703	3.61	10	17.8
tol-0022	CTIO 1.5 m	506884	2.38	10	17.8
ren-0031	Texas 2.1 m	514539	6.29	10	17.6
bph70	Hawaii 0.6 m	526387	6.37	10	17.8
a19	Australia 1.0 m	548886	3.82	10	17.9
ren-0033	Texas 2.1 m	602343	6.34	10	17.7
s4238	SA 1.0 m	748334	4.92	10	17.7
ren-0035	Texas 2.1 m	773450	6.36	10	17.8
bph71	Hawaii 0.6 m	785910	6.57	10	17.7
ren-0037	Texas 2.1 m	859883	5.50	10	16.3
bph72	Hawaii 0.6 m	872200	6.55	10	17.0
s4243	SA 1.0 m	920841	5.03	10	17.4
maw-0003.....	Texas 0.9 m	943282	7.15	10	17.5
bph73	Hawaii 0.6 m	958367	6.68	10	17.7
a26	Australia 1.8 m	974845	0.69	10	16.6
s4246	SA 1.0 m	1007844	4.80	10	17.2
maw-005	Texas 0.9 m	1029975	7.09	10	17.5
bph74	Hawaii 0.6 m	1044970	6.48	10	17.4
a28	Australia 1.8 m	1065867	3.50	10	17.2
s4250	SA 1.0 m	1095867	4.55	10	16.2
maw-0007.....	Texas 0.9 m	1115228	6.56	10	15.6
bph75	Hawaii 0.6 m	1131343	6.43	10	16.3
s4253	SA 1.0 m	1187911	2.68	10	16.7
maw-0010.....	Texas 0.9 m	1201876	7.33	10	17.5
maw-0012.....	Texas 0.9 m	1287638	7.45	10	17.7
maw-0014.....	Texas 0.9 m	1379291	7.33	10	17.7
s4256	SA 1.0 m	1443938	3.37	10	17.6
maw-0016.....	Texas 0.9 m	1473164	3.89	10	17.7

NOTE.—T_z = 2,447,229.774919 (BJED), the run start time of ren-0018. The magnitudes are derived relative to standard star observations obtained at each site and are average magnitudes for each run.

the footsteps of Winget et al. (1994) and employ the units "mi," "ma," and "mp" (see Winget et al. 1994 for explicit definitions). Modulation intensity (mi) is a linear representation of the fractional intensity of modulation. We find that the modulation intensities we observe in light curves are most conveniently expressed in units of mmi (1×10^{-3} mi), where 1 mmi $\approx$ 1 mmg. We present our FTs most conveniently in units of modulation amplitude (1 mma = 1×10^{-3} ma) or modulation power (mp = [ma]^2 and 1 μmp = 1×10^{-6} mp).

3. ANALYSIS

We begin our analysis with a visual examination of the WET light curve (Fig. 1). The high-frequency variations are obvious, but the most striking characteristic is the large range of relative amplitudes present. Such large-scale amplitude modulation may introduce significant artifacts into the FT (Provencal 1994). Indeed, the power spectrum of the entire WET data set (Fig. 2) is dominated by a complex band centered at 680 μHz, some of which may be amplitude modulation artifacts. The spectral window is given in the lower right panel.

3.1. *The Influence of the Outbursts*

Our standard reduction methods assume a variable source that maintains a constant mean magnitude, not the optimum model for this object, but the best available technique to study high-frequency modulations. If a high-frequency variation present in PG 1346+082's light curve has the form

$$f = f_0 \sin(w_0 t + \phi_0), \quad (1)$$

with f_0, w_0, and t_0 constant, it will be superposed on outbursts with ranges of $\approx$2 mag (Fig. 3). The resulting FT will be an analytical nightmare, containing numerous peaks with frequency separations characteristic of the amplitude

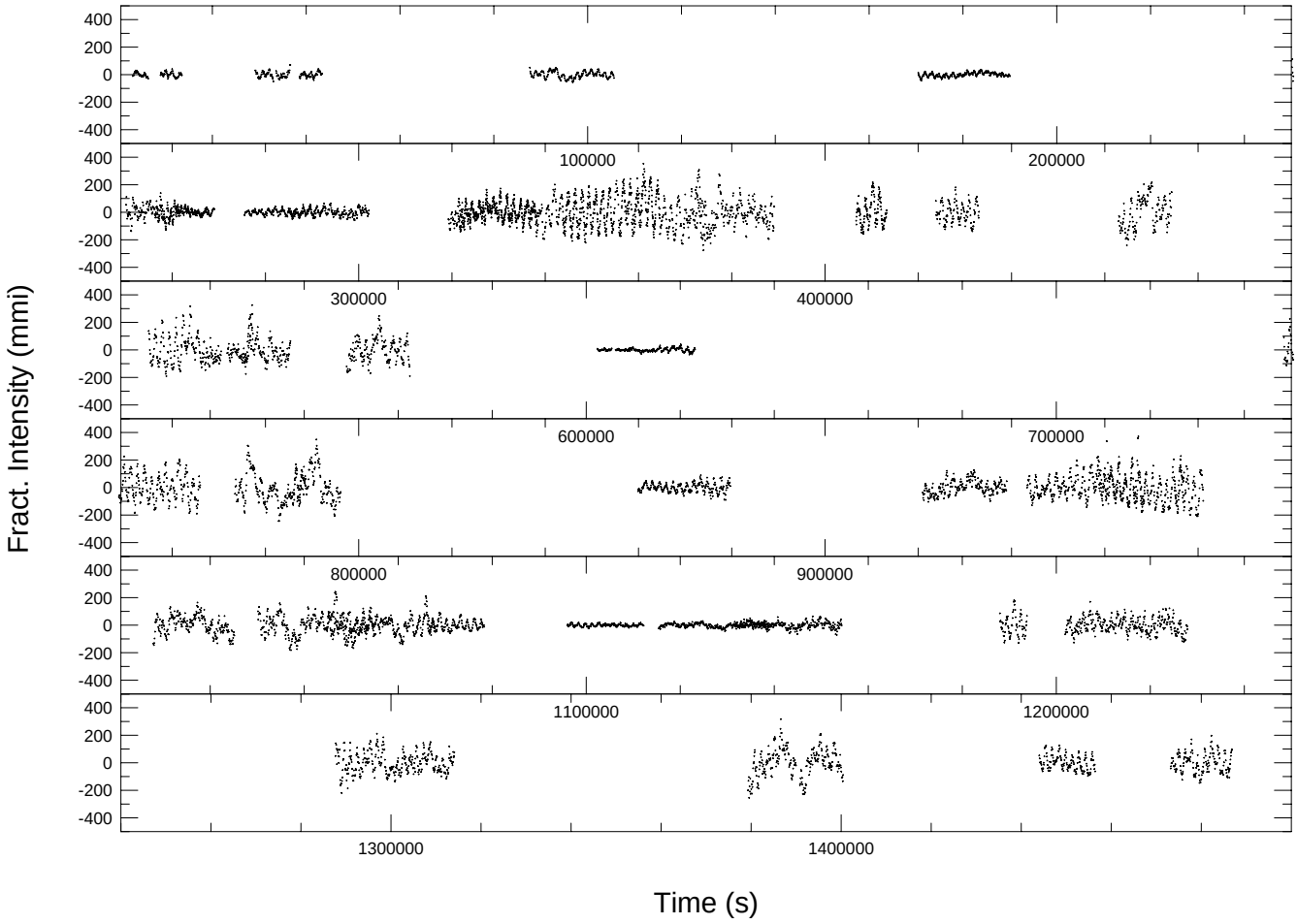

FIG. 1.—Reduced light curve of PG 1346+082 (CR Boo) obtained during XCOV I in 1988 March. We removed the large-magnitude variations. The dominant 679 μHz variation displays large-amplitude changes.

modulation timescale (Provencal 1994) that are not astrophysical in origin. On the other hand, if we allow f_0 to vary as a function of time, as in Figure 3, the FT will remain unaffected.

To test which case best describes PG 1346+082's behavior, we measure the 680 μHz and 1360 μHz peaks' relative amplitudes as a function of time (Fig. 4), choosing the number of measured points to maximize both the FT resolution and the sampling of PG 1346+082's magnitude distribution. Both the 680 μHz and 1360 μHz bands have their highest relative amplitudes when the system is dim and their lowest amplitudes when the system is bright (compare Fig. 4 with Fig. 3), suggestive of a constant physical amplitude variation superposed on a variable background. If this is true, we can predict the change in relative amplitude as a function of magnitude. During the WET run, PG 1346+082 varied from $m_b \approx 17.4$ to $m_b \approx 15.3$, producing a factor of 7 change in flux. The 680 μHz band's highest relative amplitude is 89.7 ± 2.0 mma and the lowest is 11.3 ± 1.5 mma, a decrease of a factor of 8, consistent with the hypothesis that the 680 μHz power represents a constant-amplitude variation viewed against a fluctuating background.

Our amplitude modulation investigation makes it clear that Figure 2 contains artifacts, thwarting our identification of peaks representing actual phenomena occurring in PG 1346+082. We point out that an analysis of PG 1346+082 published in 1988 (Provencal et al. 1988), identifying at least 13 separate frequencies, does not adequately solve the amplitude modulation problem. To resolve such complicated problems, we are sometimes forced to make simplifying assumptions. To simplify this problem, in the following discussion we assume that one physical configuration applies to this system in low state and another configuration applies in high state, dividing the data into high and low states by estimates of overall magnitude. In essence, we artificially choose and maintain a constant background flux by including in our separate FTs only light curves of similar mean magnitudes, thereby minimizing amplitude modulation.

3.2. *The Low-State Power Spectrum*

Nature is sometimes capricious, and despite W87's observation that PG 1346+082 is in high state over 70% of the time, the system remained in low state throughout most of our run. We present select regions of the low-state FT in Figure 5. The complex 680 μHz power band presented in Figure 2 is now resolved and contains only two frequencies, 679.670 ± 0.02 μHz (1471.30 ± 0.05 s) at a fractional amplitude of 55.4 ± 0.6 mma (hereafter ν_{L1}) and 669.887 ± 0.04 μHz (1492.79 ± 0.1 s) at 31.9 ± 0.6 mma (hereafter ν_{L2}). All remaining features are artifacts of the spectral window. We

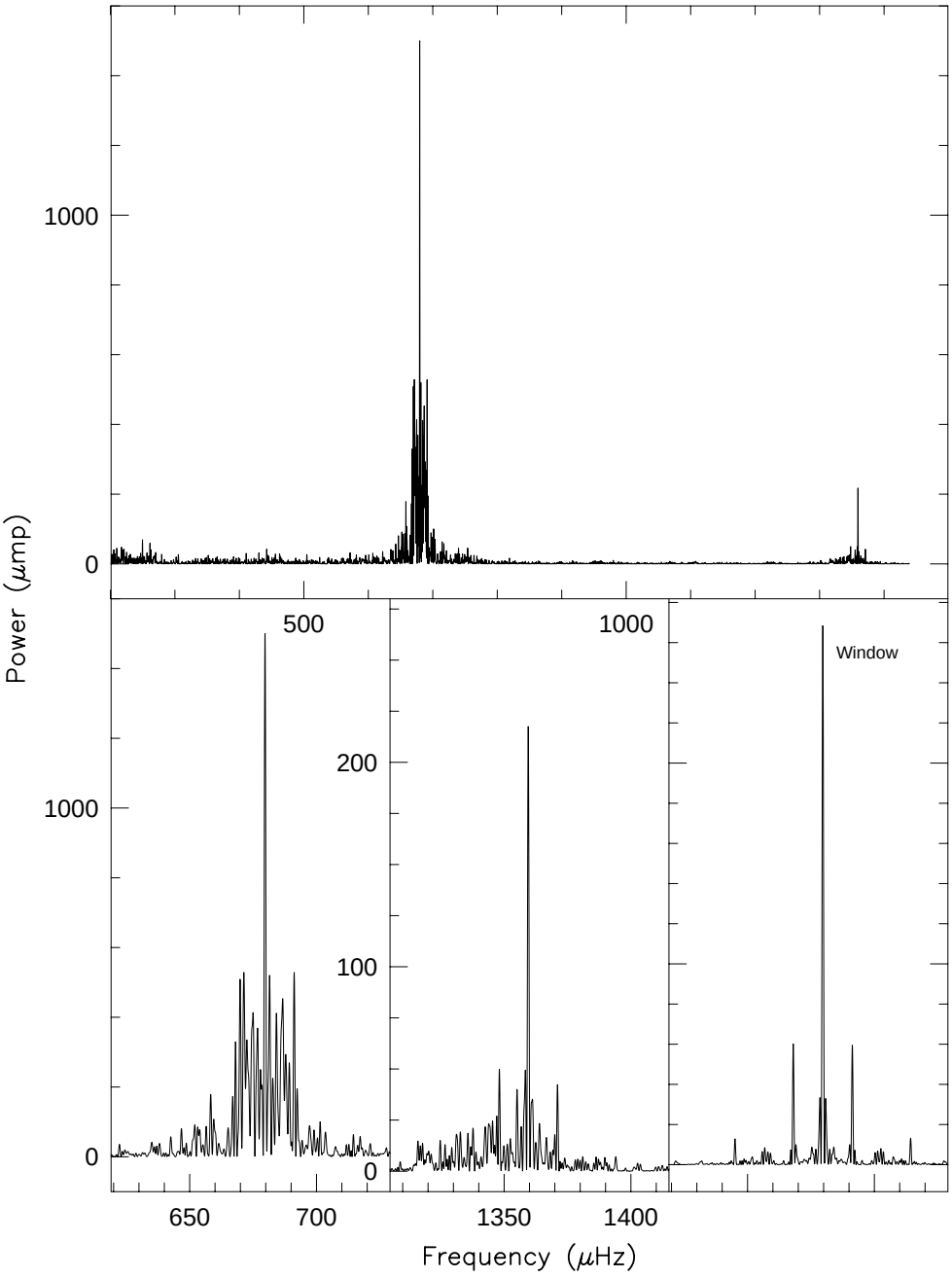

FIG. 2.—Fourier transform of the entire WET light curve. Enlargements of the spectral window and the 679 μHz and 1359 μHz regions are displayed in the lower panels.

also find power at 1359.58 $\pm$ 0.01 μHz (735.522 $\pm$ 0.005 s), the first harmonic of ν_{L1} (hereafter $2\nu_{L1}$). This is a single, isolated peak, with no evidence for a harmonic of ν_{L2}.

We corroborate W87's report of flickering in PG 1346+082's low-state light curve by examining FTs of the object obtained on two consecutive nights (Fig. 6). Both light curves are at similar low-state magnitudes, are of equal length, and are taken with the same telescope and instrument. We find significant, nonrepeating, high-frequency power, a classic signature of flickering (Warner & Robinson 1972).

3.3. *The "High-State" Spectrum*

Before proceeding with a discussion of our "high-state" FT, we must clarify our definition of the term "high." PG 1346+082 can reach a maximum brightness of 13.6 (m_b) and did brighten several times during our run. However, the system reached only $m_b \approx 15.3$, far below maximum. Our high-state data do not represent true high state for PG 1346+082, but rather the highest brightness attained during this run.

Our high-state power spectrum (Fig. 7) contains an unresolved power band at 673 μHz, shifted 7 μHz from the low-state power band, as well as a series of complex harmonics not detected in the low-state FT. We find two dominant peaks in the fundamental band, at 672.99 $\pm$ 0.04 μHz (1485.9 $\pm$ 0.1 s), with a relative amplitude of 13.8 $\pm$ 0.3 mmas (ν_{H1}), and 686.12 μHz (1457.5 $\pm$ 0.1 s) at 13.7 $\pm$ 0.4 mmas (ν_{H2}), both incommensurate with the low-state results, although we note that ν_{L1} lies almost exactly in the

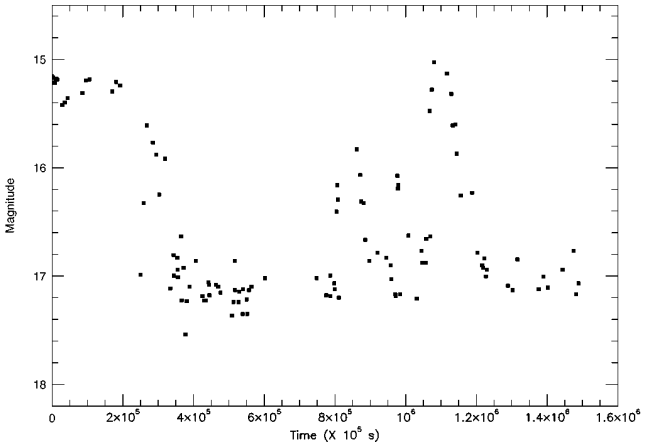

FIG. 3.—White-light magnitude of PG 1346+082 during the 1988 WET run. These magnitudes are calculated via standard star observations performed at each site. Data below $m = 17$ are included in the low-state FT, while all data above ≈ 16 are included in the high-state FT. Intermediate light curves are discarded.

middle of these two peaks. We place upper limits of approximately 5 and 7 mma for v_{L1} and v_{L2}, respectively. Since PG 1346+082 remained dim through most of the run, the high-state data are sparse, and the spectral window (Fig. 7) is significantly degraded (compare with Fig. 5). The two dominant high-state peaks are part of the same alias structure (compare their frequency separation with the alias spacing

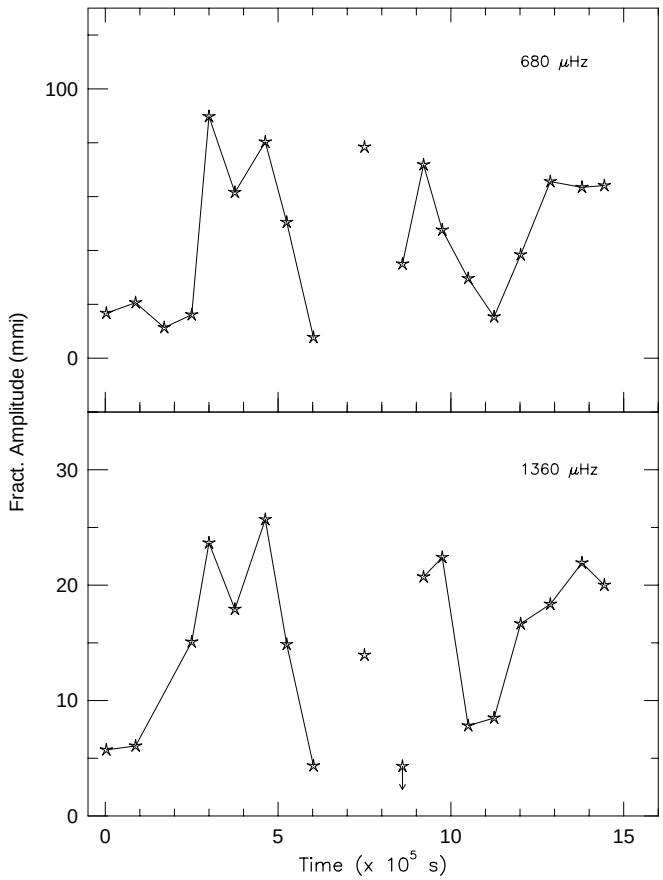

FIG. 4.—Relative amplitudes of the 679 μHz and 1360 μHz power during WET. Compared with Fig. 3, the amplitudes are high when PG 1346+082 is dim, and low when the system is bright.

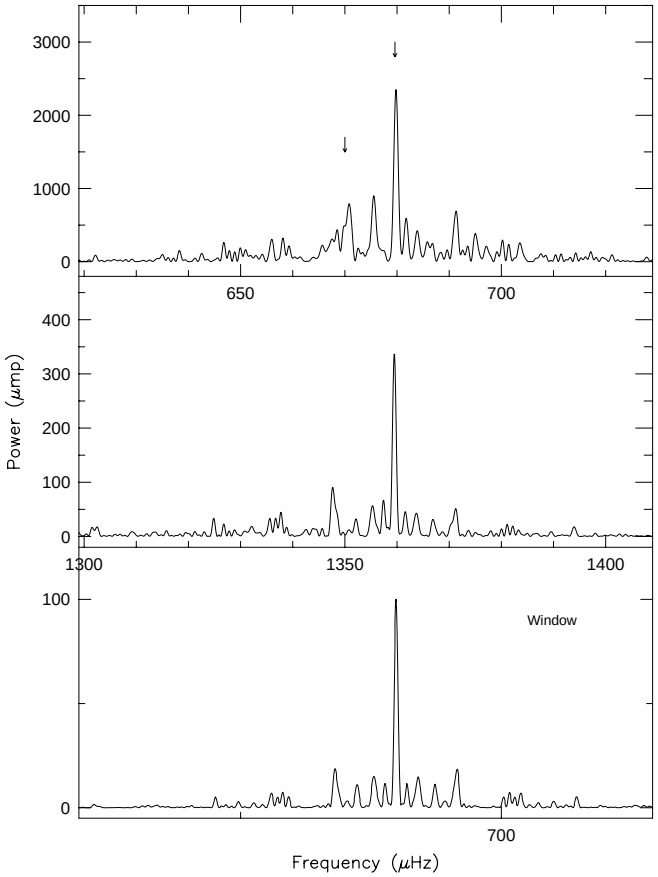

FIG. 5.—Low-state power spectrum of PG 1346+082. The fundamental band is consistent with two frequencies, at 679.67 μHz and 669.89 μHz (*arrows*). The first harmonic region, displayed in the second panel, contains a single peak at 1359.58 μHz. The spectral window is given in the third panel. Note the changes in y scale to accommodate the dynamic range.

in the spectral window), and we cannot determine which is real.

Harmonics can arise in an FT from two sources: as independently excited variations in their own right, or pulse

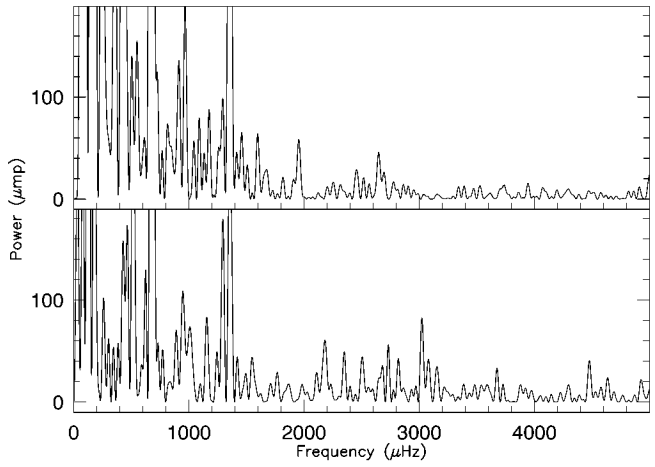

FIG. 6.—Power spectra of two consecutive nights of data of PG 1346+082. Each run is at similar magnitude, equal length, and taken with the same telescope and photometer. We find significant, nonrepeating, high-frequency power in each FT. Note the continuous presence of power at 680 μHz and 1359 μHz.

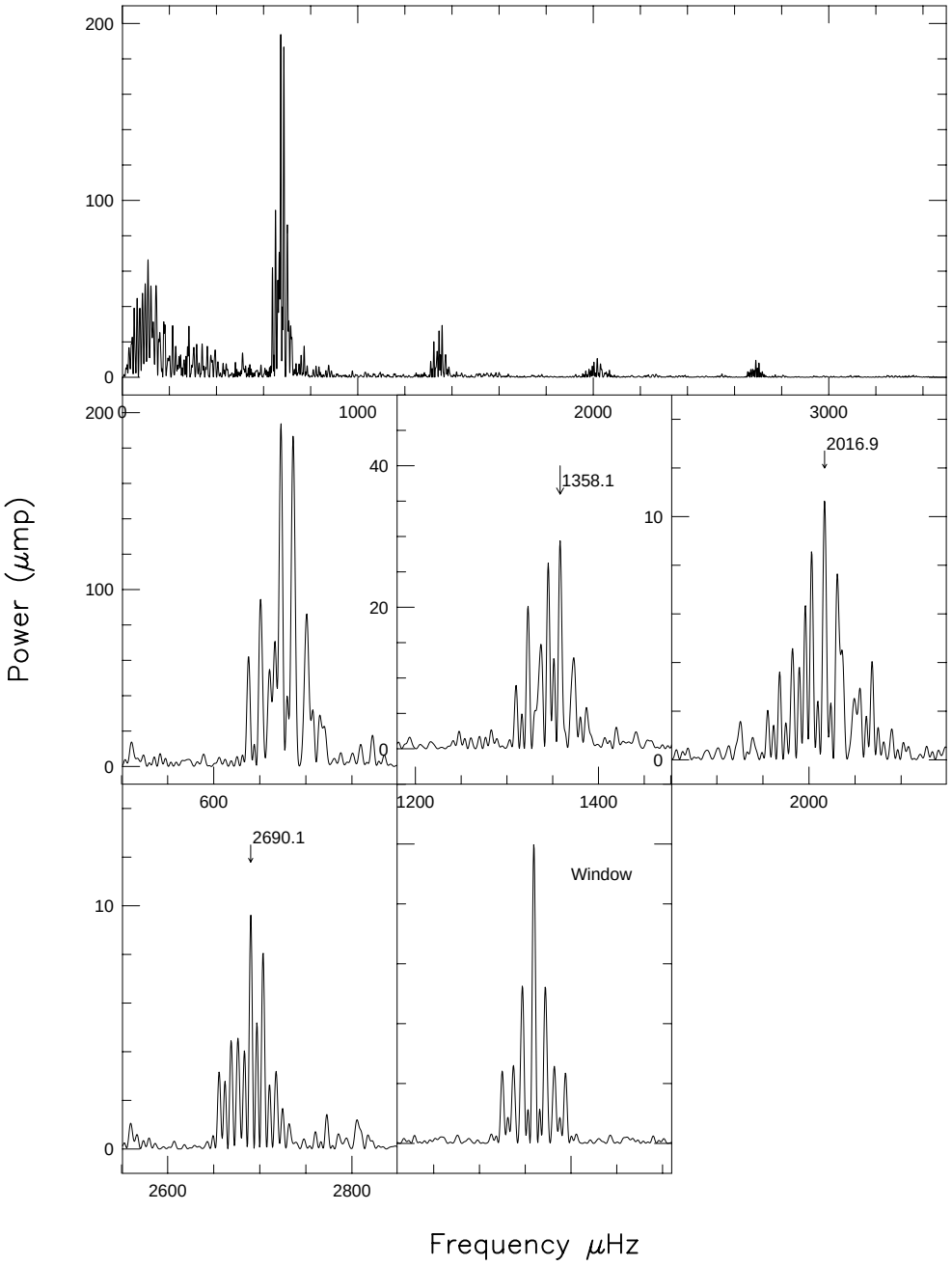

FIG. 7.—High-state power spectrum of PG 1346+082

shape distortions of a nonsinusoidal fundamental frequency (Provencal et al. 1995). If we assume the second case is true for PG 1346+082, we can use the high-state harmonics, albeit complicated by alias structure themselves, to help identify the 673 μHz band's unresolved components. The largest peak in the first harmonic power band is 1358.1 $\pm$ 0.3 μHz (6.3 mma), corresponding to a fundamental frequency of 679.05 μHz (1472.6 s), incommensurate with any power we find in the high-state 673 μHz band. The next largest peak in this region is 1345.1 $\pm$ 0.3 μHz (5.1 mma), the harmonic of ν_{H1}. Again, 1358.1 μHz and 1345.1 μHz are aliases of each other, so we cannot chose which of the peaks is real. We also cannot rule out a possible harmonic of ν_{H2}.

The situation improves as we proceed outward to higher harmonics and the corresponding frequency separation between the harmonics of ν_{H1} and ν_{H2} increases. The second harmonic region has a large peak at 2016.9 $\pm$ 0.4 μHz (3.2 mma), consistent with the second harmonic of ν_{H1}. We do not find significant power at 2058 μHz, the second harmonic of ν_{H2}. The peaks in the third and fourth harmonic regions, 2690.1 $\pm$ 0.3 μHz (3.1 mma) and 3359.9 $\pm$ 0.3 μHz (1.6 mma), again correspond to harmonics of ν_{H1}. We place upper limits of 0.7 mma and 0.4 mma for third and fourth harmonics of ν_{H2}.

The harmonics strongly support ν_{H1} as a fundamental high-state frequency. However, when compared with its spectral window (Fig. 7), the high-state 673 μHz band clearly contains additional, unresolved frequencies. We previously demonstrated the dependence of this power band's relative amplitude on system magnitude. The lack of signifi-

cant power at either ν_{L1} or ν_{L2} further illustrates a similar dependence of frequency structure on system magnitude.

3.4. *Phase Stability of the* 679 μHz *Variation*

We have identified, to the best of our current ability, the frequencies present in PG 1346+082's FT during low and high states. Our next task is to determine the physical origin of the observed frequencies. Variations stable in frequency and phase are hallmarks of orbital motion, stellar rotation, or pulsation, less stable periodicities are more likely due to accretion effects. The identification of a stable clock within any AM CVn system is something notoriously difficult to accomplish (Provencal et al. 1995; Patterson et al. 1992), and it is made more complicated by PG 1346+082's outbursts. The traditional method of phase analysis is the $O-C$ diagram, a series of data points illustrating a variation's behavior relative to an ephemeris (Kepler et al. 1991). An $O-C$ diagram requires the identification of an isolated, fully resolved peak to produce reliable results. Measuring the phase of power that is not stable in frequency and amplitude will not produce meaningful results.

Our analysis to this point demonstrates that, in the strictest sense, we cannot identify a single variation that maintains the same frequency and amplitude throughout our entire data set. Must we conclude that no stable variation exists in PG 1346+082? The answer is no. We have shown PG 1346+082 to be a complex variable, with large-scale outbursts modulating the relative amplitudes and frequencies of the short-period variations. The question we should consider is not the continuous presence of an enduring peak in an FT, but the existence of an underlying stable clock within the system, hidden beneath the outbursts.

Our best hope of locating an underlying clock in PG 1346+082 lies with our low-state data and the dominant 679.670 μHz peak (ν_{L1}). Unfortunately, because the outbursts result in coverage gaps, we cannot resolve ν_{L1} and ν_{L2} using any subset of the low-state data. Therefore, we cannot calculate a standard $O-C$ diagram for either variation. We can, however, use $2\nu_{L1}$, which is a single isolated peak in every low-state FT. We calculated a rigorous $O-C$ diagram (Fig. 8) for this frequency, finding timings consistent with a constant phase over the 2 week time span of our observations. If we assume $2\nu_{L1}$ is a pulse-shape harmonic, we can extend its phase stability to include ν_{L1}. We can also convincingly test ν_{L1}'s general phase stability by calculating the best nonlinear least-squares fit 679.670 μHz sinusoid (Press et al. 1987) to our low-state data and simply plotting this sinusoid over the light curve. We would have liked to present the entire light curve with the sinusoid superposed,

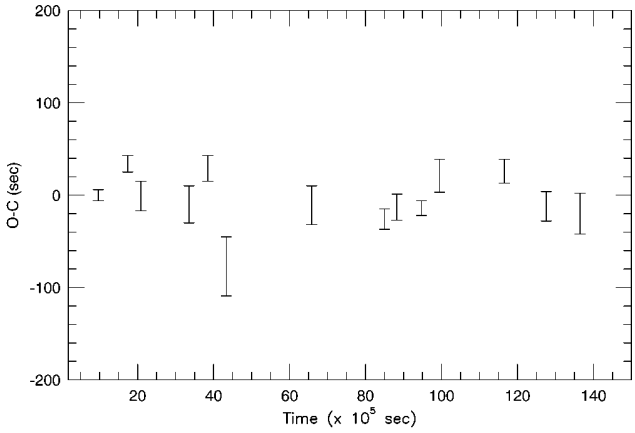

FIG. 8.—$O-C$ diagram (observed times of maxima minus calculated times) for 1360 μHz during WET run. These timings are best fit by a straight line.

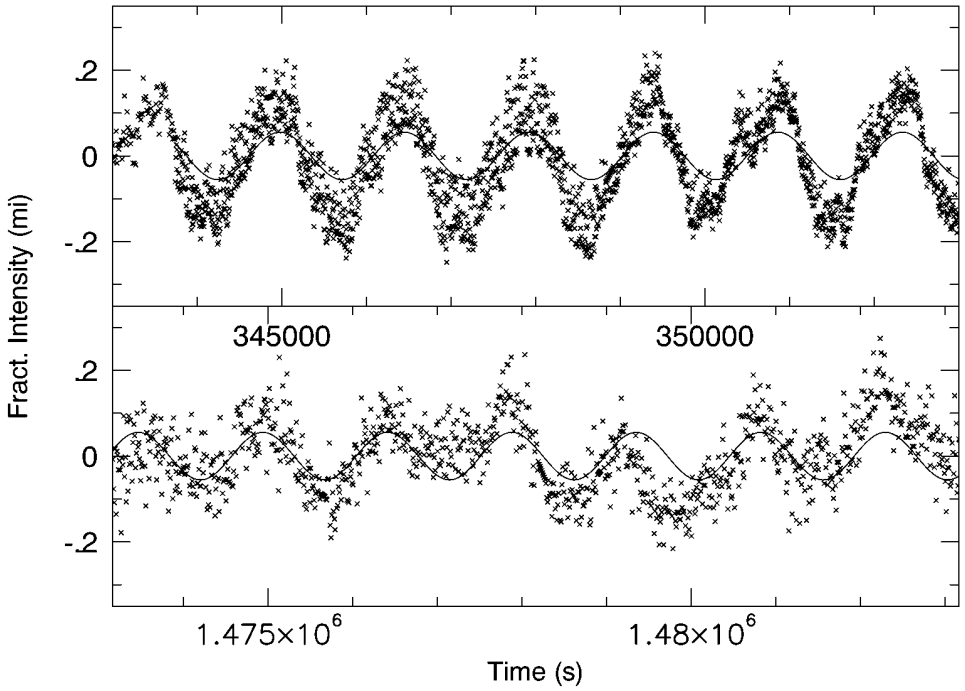

FIG. 9.—Best-fit sinusoid, $\nu = 679.67$ μHz, plotted over the low-state light curve. These panels show the fit at the beginning and end of the run, demonstrating the 679.67 μHz variation's coherency over WET's 2 week time span, despite several small system outbursts.

but this was not practical. As a compromise, Figure 9 presents this demonstration at the beginning and the end of the low-state light curve. The times of maxima/minima remain constant, illustrating the phase stability of ν_{L1} over the 2 week run. This is an extremely interesting result; our low-state data set was interrupted by PG 1346+082's excursions to higher brightness, during which ν_{L1} disappears, yet returns with its original phase after outburst.

4. DISCUSSION

Our analysis of PG 1346+082's photometric behavior has yielded some significant results, including the identification of two low-state frequencies at 679.67 μHz and 669.89 μHz, one of which is demonstrably coherent over at least a 2 week timescale. Moreover, we find a correlation between the short-period power's relative amplitude and frequency structure and overall system brightness, and note the appearance of high-order harmonics at brighter magnitudes.

Our results allow us to draw interesting comparisons between PG 1346+082 and other family members, particularly CP Eri and V803 Cen (O'Donoghue, Menzies, & Hill 1987), supporting the conclusion that the same basic model applies to all such systems. Overall, the power spectrum of PG 1346+082 shows a resemblance to CP Eri (Fig. 10): a fundamental power band and first harmonic in low state,

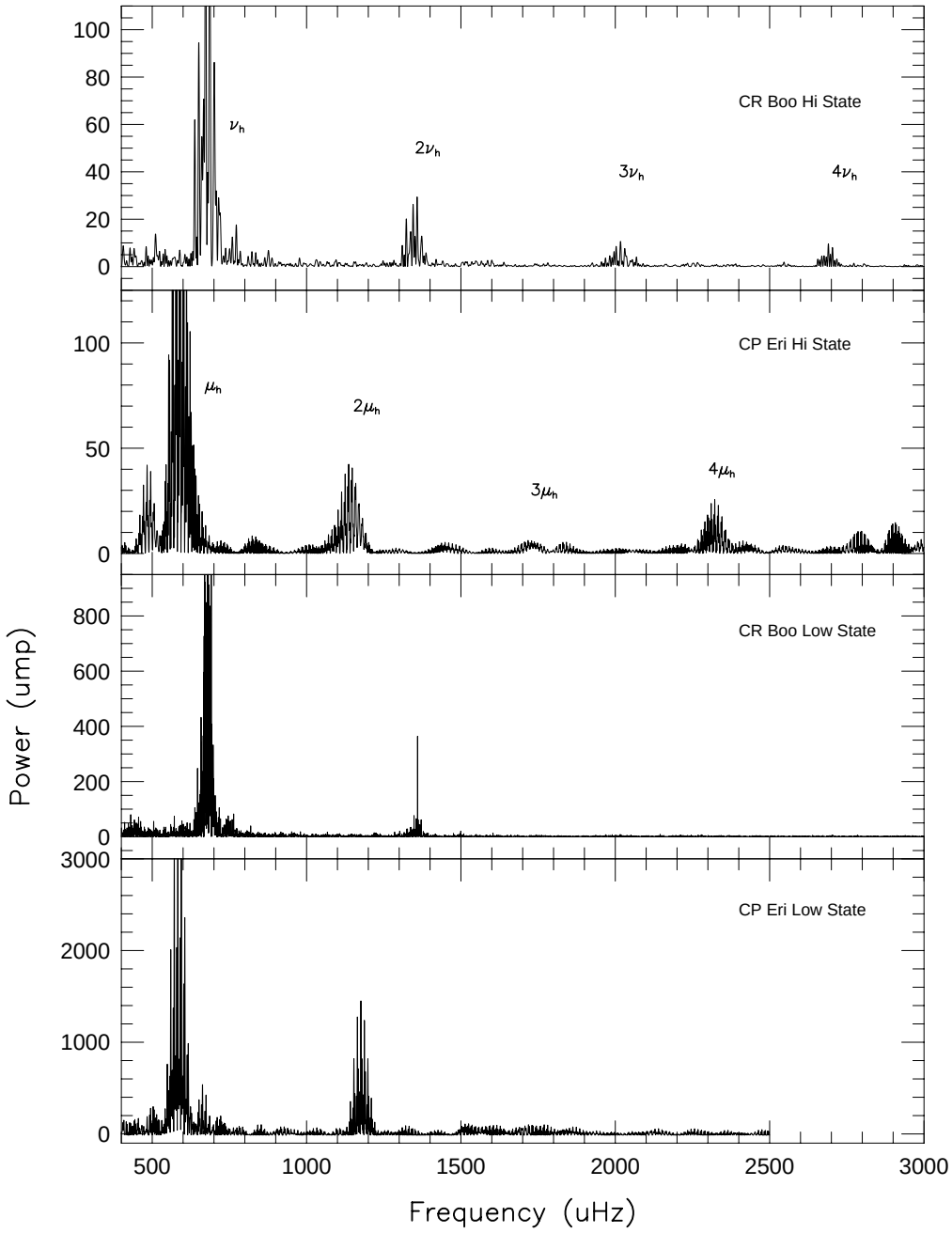

FIG. 10.—Power spectra of CR Boo and CP Eri in high and low state. These objects show behavior characteristic of the AM CVn family, particularly the dwarf-novae systems.

and a change in the fundamental band's frequency structure, coupled with the appearance of higher order harmonics, in high state. CP Eri also exhibits the same relative amplitude dependence we observe in PG 1346+082 (Provencal 1994).

This bright state pattern of a fundamental coupled with a series of harmonics is also followed by EC 15330−1403 (O'Donoghue et al. 1994), the newest AM CVn star, with photometric periods and spectra similar to the prototype AM CVn. The case is less clear for AM CVn itself, where we find numerically related peaks in the power spectrum but the hypothetical fundamental frequency has never been observed (Provencal et al. 1995).

While we are confident that the interacting binary model is a starting point for all members of this family, some curious details require further explanation. Figure 11 presents the average pulse shapes of PG 1346+082 (low state), AM CVn, CP Eri (low state), and the helium white dwarf pulsator GD 358 (Provencal et al. 1995). We have just shown that CP Eri and PG 1346+082 exhibit the same frequency and relative amplitude behavior in their FTs, yet PG 1346+082's pulse shape is quite unlike CP Eri's. In contrast, CP Eri's low-state pulse shape is remarkably similar to AM CVn's, an object believed to be in constant outburst. These discrepancies are probably due to ill-understood differences in disk structure requiring further study.

The basic model for AM CVn stars contains two white dwarfs of extreme mass ratio transferring material via an accretion disk. The range of general photometric and spectroscopic behavior over the family is explained as differences in orbital separation and mass transfer rates. One popular variation of this model ascribes the photometric and spectroscopic properties to the same type of physical phenomena observed in the SU UMa subclass of dwarf novae (see Warner 1995 for an in-depth review). In the superhump model, tidal stresses compel the disk to assume an elliptical shape, which then precesses. Photometric variations are observed at the orbital period ($P_{\rm orb}$) and the superhump period (P_s), where $1/P_s = 1/P_{\rm orb} - 1/P_{\rm prec}$, and $P_{\rm prec}$ is the precession period.

If we assume the low-state frequencies ν_{L1} and ν_{L2} represent PG 1346+082's orbital and superhump frequencies respectively, we arrive at a precession period of $P_{\rm prec} = 1.18$ days. We point out that this is also the timescale over which PG 1346+082 underwent small outbursts during our run.

While superhumps are observed primarily during outburst in hydrogen-rich systems, the helium disks in AM CVn systems, because of their ultrashort orbital periods and extreme mass ratios, can expand into a region where tidal resonance with the secondary occurs. Tidal dissipation in the disk's outer edges maintains the entire disk in the high-viscosity state required for dwarf nova outbursts. Warner (1995) outlines a series of steps to obtain values for the

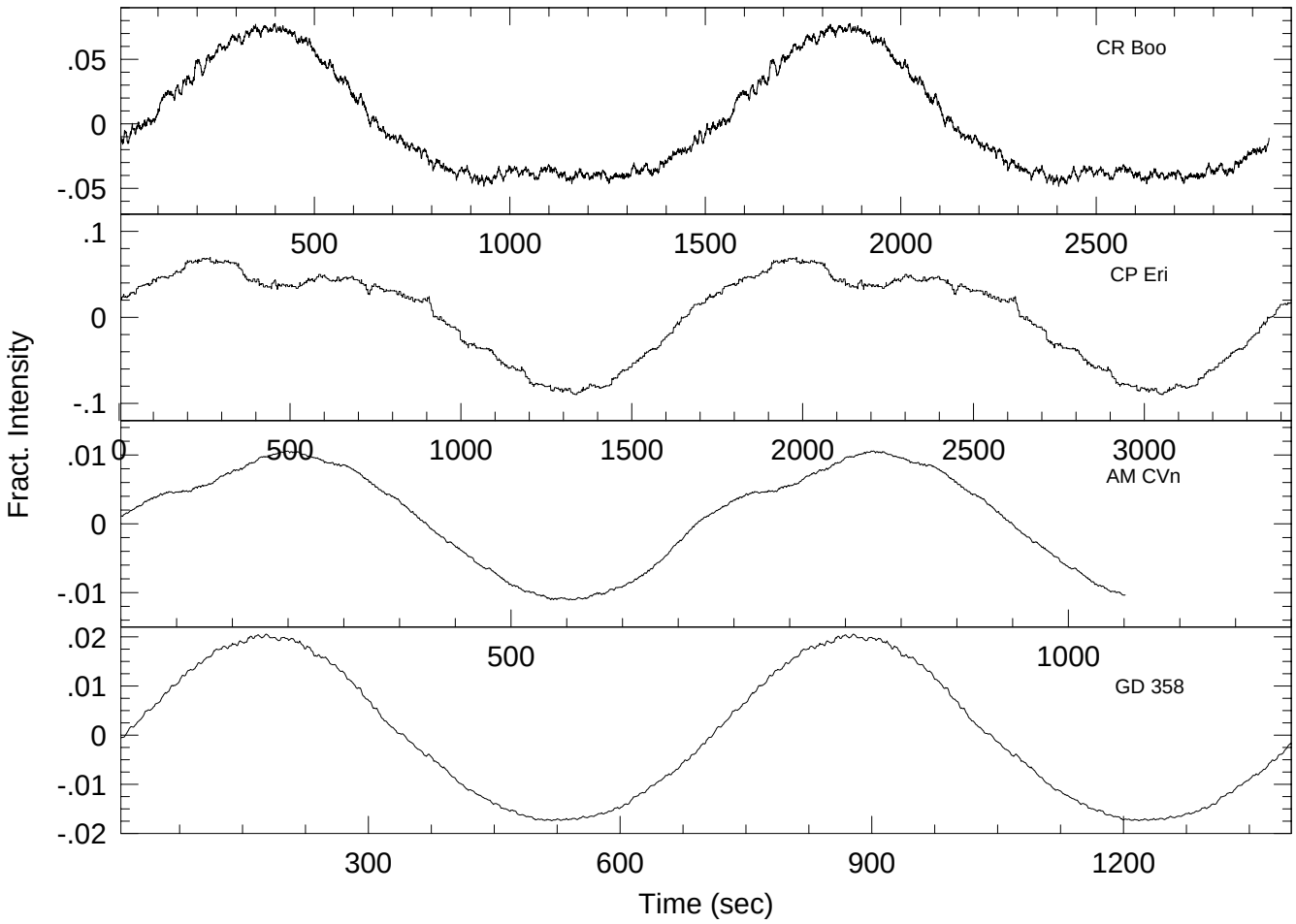

FIG. 11.—The 679 μHz pulse shape, compared with the pulse shapes of dominant photometric variations of AM CVn, the prototype IBWD, and GD 358, a nonradially pulsating DB white dwarf.

masses of the primary and secondary components. The author assumes the secondary fills its Roche lobe and the mass transfer rate is large enough to drive the low-mass He secondary out of thermal equilibrium, resulting in a semi-degenerate object. Proceeding with these assumptions and following the steps outlined by Warner (1995), using

$$\frac{P_{\rm prec}}{P_{\rm orb}} = A\,\frac{1+q}{q}\,, \tag{2}$$

where $A \approx 3.73$ for $q \leq 0.1$ (Warner 1995), we arrive at an extreme mass ratio of 0.057, a primary mass of 1 $M_\odot$, and a secondary mass of 0.057 $M_\odot$, within the range expected for this system.

Further analysis of PG 1346+082 will have much to say concerning the outburst mechanism in AM CVn systems. If both the short-period modulations and the outbursts originate in the disk, we must confront the observation that the relative amplitude of this power actually decreases when the disk is brightening, arguing strongly that the outburst swamps the source and does not cause the source itself to brighten. The observed frequency changes demonstrate that the source is affected, however. We note again that $\nu_{\rm L1}$ lies almost exactly between $\nu_{\rm H1}$ and $\nu_{\rm H2}$. If we consider this frequency change as a Doppler shift rather than the emergence of new power, we find velocities of $\approx$3000 km s^{-1}, not unreasonable for this system. Details of harmonic behavior through an outburst, coupled with the observed frequency changes, may actually locate both the origin of the outbursts and the short-period source.

While the outburst may take place in a localized region of the disk, such as the boundary layer, we cannot rule out the accreting white dwarf as a possible source of some high-frequency variations. It is not unusual for the underlying white dwarf to be observable during low state (Sion et al. 1995). Disk outbursts would subsequently swamp any modulations arising on the white dwarf. We may be dealing with a tidally locked, or nearly so, system, explaining the frequency changes as white dwarf in low state, and accretion disk in high state.

The appearance of high-order harmonics in the power spectra of dwarf nova–like AM CVn stars during outburst is certainly linked with the outburst mechanism. The harmonics offer a tantalizing opportunity to probe a helium disk through an outburst. As stated previously, harmonics can arise from two sources. A purely sinusoidal variation will produce no harmonics in an FT. A nonsinusoidal variation will, however, and these harmonics can be used as a measure of the pulse shape of the fundamental frequency. If the harmonics in PG 1346+082 are pulse-shape harmonics, their appearance in high state translates to a change in the pulse shape of the fundamental frequency and, hence, a change in disk shape. In this case, their time-dependent behavior will provide a sensitive probe of disk shape through an outburst. The second possibility is that these harmonics represent independent physical modulations in their own right. PG 1346+082's effective temperature in high state (W87) is within the temperature range where helium is partially ionized, providing an efficient mechanism to drive pulsations within the disk. Disk oscillations can be used to pursue details of disk structure, stratification, and composition, much as nonradial pulsations probe the details of white dwarf interiors (Winget et al. 1994). Moreover, orbital resonances will be more easily excited, and as such, the shorter period harmonics will originate closer to the white dwarf. Investigation of their time-dependent behavior, for example, which appears first at outburst initiation, or of whether a pattern of amplitude variations occurs, could trace not only disk structure but also mass transfer through the disk, giving us direct measurement of viscosity. In either case, the dwarf nova–like AM CVn stars offer a unique laboratory to study accretion disks, and PG 1346+082 is worthy of further study.

5. CONCLUSIONS

Our analysis of WET observations of PG 1346+082 identifies two frequencies in the low-state power spectrum, at 669.89 μHz ($\nu_{\rm L2}$) and 679.67 μHz ($\nu_{\rm L1}$), which we tentatively identify as possible superhump and orbital frequencies, respectively. The frequency $\nu_{\rm L1}$ is coherent over the 2 week run, despite the system suffering several small outbursts. This is the first demonstration of a phase-coherent photometric variation within any dwarf nova–like AM CVn system. We also uncover the unexpected dependences of the short-period power's relative amplitude and frequency structure on overall system magnitude. While the observed amplitude dependence can be explained as a constant-amplitude source superposed on a variable background, we have no solid explanation for the observed frequency changes.

Much work remains before we can understand the AM CVn family. Our analysis of PG 1346+082 has produced a list of observational features which must be reproduced by any appropriate model:

1. A fundamental variation and its first harmonic in low state.
2. The emergence of higher order harmonics at brighter magnitudes.
3. The fundamental "band" may contain multiple frequencies.
4. Inverse dependence of the amplitude of the short-period variations with magnitude.
5. Changing frequency structure with magnitude.

We have also compiled a wish list of theoretical and observational work required to expand the overall model. Detailed theoretical understanding of disk oscillations is critical to access information carried by the harmonics. If the harmonics are strictly pulse-shape artifacts, time-resolved observations over several outbursts will provide detailed maps indicating changes in disk structure. During our observations, PG 1346+082's outbursts occurred on the same timescale as the hypothetical precession period and did not reach maximum brightness. Yet the amplitude of the supposed superhump period, $\nu_{\rm L2}$, actually decreased as the system brightened. These minioutbursts may signify failed attempts to create and sustain an organized disk. Observations at maximum brightness, with sufficient time base and coverage to resolve the relevant frequencies, are needed. If the dominant true high-state frequency is 669.89 μHz, this would go a long way toward confirming the superhump model. Obtaining such data requires extra persistence from observers. Unlike its better behaved cousin AM CVn, this system does not maintain a constant mean magnitude, and its outbursts are unpredictable. However, PG 1346+082 is one of the brighter AM CVn stars undergoing outbursts and offers a unique opportunity to study

the fluid behavior of helium in an accretion disk. Persistence will be well rewarded.

This work was supported in part by NSF grants AST 85-52456, AST 86-00507, AST 87-12249, AST 88-13572, AST 90-013978, AST 90-13368, and AST 92-17988, NASA grant NGG-50468 and National Geographic Society 3547-87. Special thanks are due to Harry Shipman for his helpful comments.

REFERENCES

Dehner, B. T., & Kawaler, S. D. 1995, ApJ, 443, 735
Faulkner, J., Flannery, B. P., & Warner, B. 1972, ApJ, 175, L79
Fontaine, G., & Wesemael, F. 1996, in 10th European Workshop on White Dwarfs (Dordrecht: Kluwer), in press
Green, R. F., Schmidt, M., & Liebert, J. 1986, ApJS, 61, 305
Kepler, S. O., et al. 1991, in NATO ASI Ser. Proc. 7th European Workshop on White Dwarfs, ed. G. Vauclair & E. M. Sion (Dordrecht: Kluwer), 143
Marsh, T. R., Horne, K., & Rosen, S. 1991, ApJ, 366, 535
Nather, R. E. 1973, Vistas Astron., 15, 91
Nather, R. E., Robinson, E. L., & Stover, R. J. 1981, ApJ, 244, 269.
Nather, R. E., Winget, D. E., Clemens, J. C., Hansen, C. J., & Hine, B. P. 1990, ApJ, 361, 309
Nather, R. E., Wood, M. A., Winget, D. E., & Liebert, J. 1984, IAU Circ., 4021
O'Donoghue, D., Kilkenny, D., Chen, A., Stobie, R. S., Koen, C., Warner, B., & Lawson, W. A. 1994, MNRAS, 271, 910A
O'Donoghue, D., Menzies, J. W., & Hill, P. W. 1987, MNRAS, 227, 347
Patterson, J., Halpern, J., & Shambrook, A. 1993, ApJ, 419, 803
Patterson, J., Schwartz, D. A., Pye, J. P., Blair, W. P., Williams, G. A., & Caillault, J.-P. 1992, ApJ, 392, 233
Press, W. H., Flannery, B. P., Teukolsky, S. A., & Vettering, W. T. 1987, in Numerical Recipes, ed. W. H. Press (Cambridge: Cambridge Univ. Press), 203
Provencal, J. L. 1994, Ph.D. thesis, Univ. Texas
Provencal, J. L., et al. 1988, Lecture Notes in Phys., 328, 296
———. 1995, ApJ, 445, 927
Provencal, J. L., Shipman, H. L., Thejll, P., Vennes, S., & Bradley, P. A. 1996, ApJ, 466, 1011
Shafter, A. W., & Szkody, P. 1984, ApJ, 276, 305
Shipman, H. L. 1996, in 10th European Workshop on White Dwarfs (Dordrecht: Kluwer), in press
Sion, E. M., et al. 1995, ApJ, 439, 957
Wade, R. A., & Ward, M. J. 1985, Interacting Binary Stars (Cambridge: Cambridge Univ. Press), 149
Warner, B. 1995, Ap&SS, 225, 249
Warner, B., & Robinson, E. L. 1972, MNRAS, 159, 101
Winget, D. E., et al. 1987, ApJ, 315, L77
———. 1991, ApJ, 378, 326
———. 1994, ApJ, 430, 839
Wood, M. A., et al. 1987, ApJ, 313, 757 (W87)